

1 Megakaryocyte and erythroblast DNA in plasma and platelets

2

3 Joshua Moss^{†1,2}, Roni Ben-Ami^{†1}, Ela Shai³, Yosef Kalish³, Agnes Klochender¹, Gordon
4 Cann⁴, Benjamin Glaser⁵, Ariela Arad^{*3}, Ruth Shemer^{*1}, Yuval Dor^{*1}

5 Affiliations:

6 ¹Department of Developmental Biology and Cancer Research, Institute for Medical Research Israel-
7 Canada, the Hebrew University-Hadassah Medical School; Jerusalem, Israel

8 ²Sharett Institute of Oncology, Hadassah-Hebrew University Medical Center; Jerusalem, Israel

9 ³Hematology Department, Hadassah-Hebrew University Medical Center; Jerusalem, Israel

10 ⁴GRAIL, LLC.; Menlo Park, California, United States of America

11 ⁵Endocrinology and Metabolism Service, Hadassah University Medical Center and Faculty of
12 Medicine, the Hebrew University; Jerusalem, Israel

13 [†] These authors contributed equally

14 ^{*} Corresponding authors: Yuval Dor, yuvald@ekmd.huji.ac.il; Ruth Shemer,
15 shemer.ru@mail.huji.ac.il; Ariela Arad, arielaar@hadassah.org.il

16

17 ABSTRACT

18

19 Circulating cell-free DNA (cfDNA) fragments are a biological analyte with extensive utility
20 in diagnostic medicine. Understanding the source of cfDNA and mechanisms of release is
21 crucial for designing and interpreting cfDNA-based liquid biopsy assays. Using cell type-
22 specific methylation markers as well as genome-wide methylation analysis, we determined
23 that megakaryocytes, the precursors of anuclear platelets, are major contributors to cfDNA
24 (~26%), while erythroblasts contribute 1-4% of cfDNA in healthy individuals. Surprisingly,
25 we discovered that platelets contain genomic DNA fragments originating in megakaryocytes,
26 contrary to the general understanding that platelets lack genomic DNA. Megakaryocyte-
27 derived cfDNA is increased in pathologies involving increased platelet production (Essential
28 Thrombocytopenia, Idiopathic Thrombocytopenic Purpura) and decreased upon reduced
29 platelet production due to chemotherapy-induced bone marrow suppression. Similarly,
30 erythroblast cfDNA is reflective of erythrocyte production and is elevated in patients with
31 Thalassemia. Megakaryocyte- and erythroblast-specific DNA methylation patterns can thus
32 serve as novel biomarkers for pathologies involving increased or decreased thrombopoiesis
33 and erythropoiesis, which can aid in determining the etiology of aberrant levels of
34 erythrocytes and platelets.

35

36

37

38

39

40

41

42

43

44

45

46

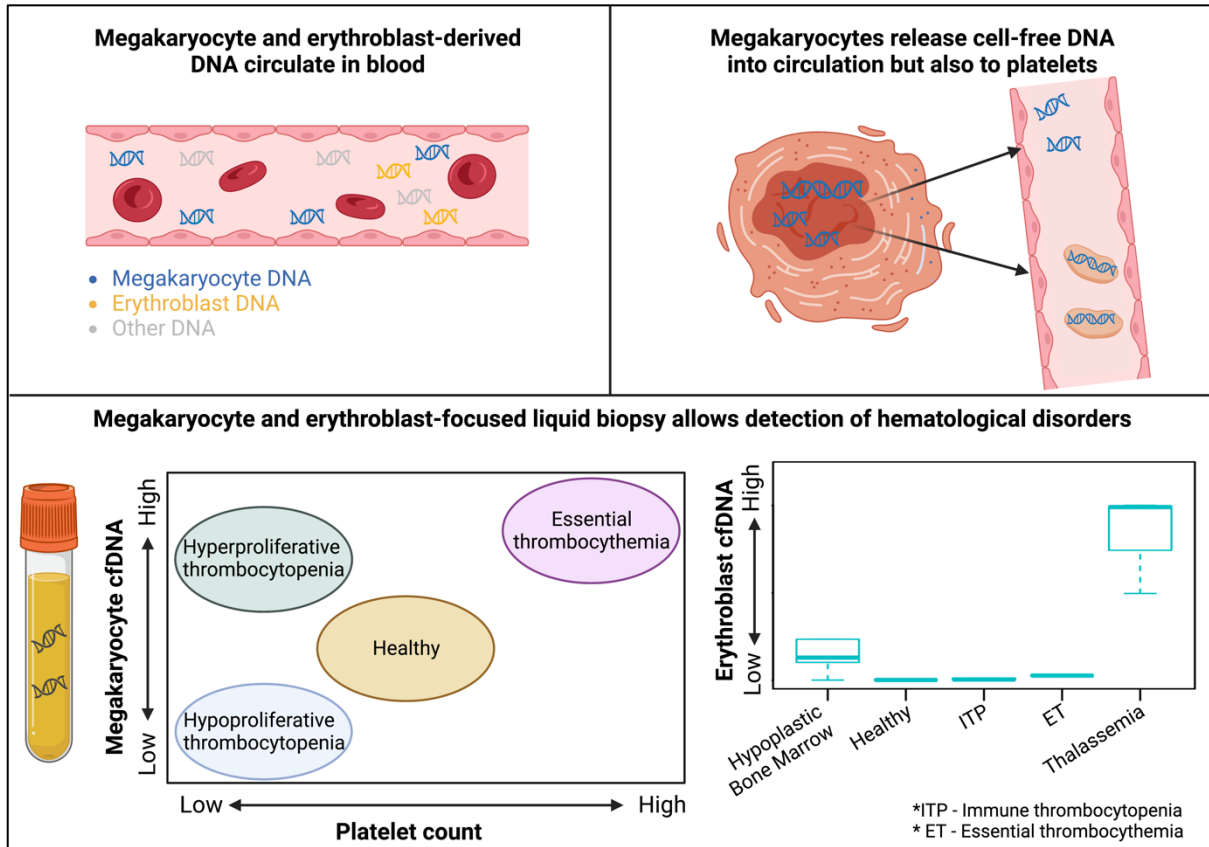
47

48

49

50 **GRAPHICAL ABSTRACT**

51



52

53 INTRODUCTION

54

55 Circulating cell-free DNA (cfDNA) molecules are thought to be released from dying cells and
56 can be used to monitor tissue turnover rates in health and disease. Fetal DNA present in
57 maternal circulation allows for detection of fetal aneuploidies¹; donor-derived DNA in the
58 circulation of organ transplant recipients provides a non-invasive marker of graft rejection²;
59 and tumor-derived mutant cfDNA allows for detection and monitoring of cancer³.

60 Accurate identification of the tissue origins of cfDNA holds great potential for sensitive
61 monitoring of turnover dynamics in specific tissues and cell types, in health and disease. DNA
62 methylation patterns provide means for determining the tissue origins of cfDNA, given the
63 extreme cell type specificity of this epigenetic mark⁴. Indeed, we and others have shown that
64 tissue-specific methylation patterns can serve as cfDNA biomarkers for elevated turnover in
65 specific tissues. For example, cardiomyocyte DNA is present in the plasma of patients
66 following myocardial infarction⁵; hepatocyte cfDNA is present in the plasma of patients with
67 liver damage⁶, and exocrine pancreas DNA is found in the plasma of patients with pancreatitis⁷.
68 Additionally, novel assays detect cancer-related methylation aberrations for early diagnosis of
69 cancer⁸. Alternative approaches for determining the tissue origins of cfDNA rely on tissue-
70 specific patterns of nucleosome positioning⁹, fragmentation, topology and size of cfDNA¹⁰.

71 More recently, patterns of histone modification in circulating chromatin fragments were used
72 to infer gene expression and hence identity of the cells that gave rise to cfDNA¹¹. Such analyses
73 of the circulating epigenome demonstrated that plasma cfDNA is mostly derived from cells of
74 hematopoietic origin, specifically neutrophils (30%), lymphocytes (12%) and monocytes
75 (11%), as well as vascular endothelial cells (~10%) and hepatocytes (1-3%)¹². However, there
76 have been contrasting reports regarding the contribution of cfDNA from erythroblasts and
77 megakaryocytes, cells which arise from two related but distinct blood lineages. Lam et al. have
78 identified genomic loci that are unmethylated specifically in erythroid cells and assessed their
79 level in cfDNA. They concluded that ~30% of cfDNA originates from erythroid cells, and that
80 anemia and thalassemia impact the level of erythroid cfDNA¹³. Consistent with this, our own
81 deconvolution of the plasma methylome suggested that erythrocyte progenitors contribute to
82 ~30% of cfDNA in healthy individuals¹². However, these studies did not take into account the
83 relative contribution of megakaryocytes to cfDNA. Sadeh et al. concluded from
84 immunoprecipitation of circulating chromatin that megakaryocytes, rather than erythroblasts,
85 are major contributors of nucleosomes to healthy plasma¹¹.

86

87 In this study, we identified definitive methylation markers that distinguish megakaryocytes and
88 erythroblasts and used these to characterize the presence of DNA from megakaryocytes and
89 erythroblasts in plasma of healthy individuals and in different pathological scenarios which
90 affect the production of platelets and red blood cells. We found that measuring megakaryocyte
91 and erythroblast cfDNA allows the detection and distinction of pathologies affecting these
92 lineages, even when not reflected in peripheral blood cell counts. Furthermore, after
93 establishing the presence of a significant amount of megakaryocyte-derived DNA in
94 circulation, we went on to question whether megakaryocyte-derived DNA reaches plasma via
95 platelets. This led to an discovery that platelets, not previously believed to contain genomic
96 DNA, do in fact contain genomic DNA, despite the lack of a nucleus.

97

98

99 RESULTS

100

101 **Methylomes of erythroblasts and megakaryocytes and their representation in healthy**
102 **plasma**

103 Due to previous reports that non-leukocyte cells of hematopoietic origin are major contributors
104 to cfDNA, we sought to evaluate the relative contribution of erythroid and megakaryocyte
105 genomes. To this end, we isolated DNA from bone-marrow erythroblasts (**Supplementary**
106 **Figure S1**) as well as multiple types of white blood cells (see methods) and performed whole-
107 genome bisulfite sequencing to obtain a genome-wide methylation profile of each cell type.
108 We also obtained previously published genome-wide methylation profiles of megakaryocytes
109 as well as common megakaryocyte-erythroid progenitors for comparison. This comparison
110 revealed multiple loci that were uniquely methylated or unmethylated in erythroblasts (1884
111 sites) and in megakaryocytes (97 sites) and could in principle serve as specific biomarkers for
112 DNA derived from these cell types (**Figure 1A-B**). The erythroblast genome was largely
113 unmethylated, in line with previous reports describing gradual genome-wide demethylation of
114 erythroid cells in mice and humans during their terminal differentiation^{14,15} (**Supplementary**
115 **Figure S2**).

116 In order to evaluate the contribution of these genomes to cfDNA, we obtained genome-wide
117 methylation profiles of purified white blood cells (WBC) and cfDNA from 23 healthy
118 individuals, sequenced at ~85 coverage¹⁶. Methylation levels of genomic regions uniquely
119 unmethylated in megakaryocytes were ~26% less methylated in cfDNA compared to WBC-
120 derived DNA (**Figure 1A**), suggesting that megakaryocyte genomes are major contributors to
121 cfDNA. In contrast, genomic regions uniquely unmethylated in erythroblasts were only ~4%
122 less methylated in cfDNA compared to WBC-derived DNA (**Figure 1B**), suggesting that
123 erythroblast genomes are minor contributors to cfDNA in healthy individuals. The fact that
124 erythroblast and megakaryocyte markers are methylated in WBC further supports the idea that
125 they originate in cells that are not present in circulation. Targeted bisulfite PCR-sequencing of
126 regions uniquely unmethylated in megakaryocytes or erythroblasts in cfDNA or blood was
127 consistent with the genome-wide analyses, demonstrating elevated levels of megakaryocyte as
128 well as erythroblast DNA in plasma as compared to whole blood (**Figure 1C-D**,
129 **Supplementary Figure S3-S4**).

130
131

132 **Platelets contain genomic DNA from MK**

133 We sought to evaluate how megakaryocyte-derived DNA reaches the plasma. Platelets are
134 products of megakaryocytes, that contain megakaryocyte-derived pre-mRNA and mRNA¹⁷ and
135 carry out splicing and protein synthesis, but do not contain a nucleus and are not thought to
136 contain genomic DNA. However it has been reported that platelets contain histone proteins¹⁸,
137 raising the possibility that they may carry some megakaryocyte DNA as well. To test this idea,
138 we isolated platelets (see methods) and performed DNA extraction (**Supplementary Table**
139 **S2**). We reasoned that DNA found in platelets could be genomic DNA of a megakaryocyte that
140 was trapped within forming platelets, or alternatively could be cfDNA from other cell types
141 that adhered to the external surface of platelets or was internalized, similar to tumor-derived
142 mRNA which has been suggested to be present in platelets of individuals with cancer^{19,20}. To
143 distinguish between these possibilities, we performed targeted bisulfite sequencing of regions
144 uniquely unmethylated in megakaryocytes in the platelet DNA concentrates. Strikingly,
145 platelet DNA was found to be mostly unmethylated at these loci (~80%), suggesting
146 megakaryocytes as the main origin of platelet DNA (**Figure 2A**). Platelet concentrates also
147 contained DNA methylation markers of leukocytes and hepatocytes, suggesting the presence
148 of some DNA from these cell types (**Figure 2A**). To distinguish between DNA associated with
149 the external surface of platelets and DNA present within platelets we treated platelet isolates
150 with DNaseI, reasoning that this enzyme would have an effect only on external DNA.
151 Strikingly, DNase treatment did not reduce the concentration of megakaryocyte DNA in
152 platelets but did eliminate leukocyte- and hepatocyte-derived DNA (**Figure 2B and**

153 **Supplementary Figure S5**), suggesting that the megakaryocyte DNA is present within the
154 platelet. Interestingly, platelet DNA is present in the form of large molecular weight DNA, in
155 contrast to nucleosome-size fragments of typical cfDNA (**Supplementary Figure S6**).
156 Notably, the total amount of DNA present in platelets ($\sim 2 \times 10^{-6}$ genomes/platelet) suggests that
157 only a small fraction ($\sim 0.1\%$) of a megakaryocyte genome DNA is present in the platelets that
158 derive from this cell (**Supplementary Table S2**).

159
160

161 **Genome-wide analysis of platelet DNA**

162 In order to confirm that platelet DNA is megakaryocyte-derived, we performed whole-genome
163 bisulfite sequencing of platelet DNA (n=3 individuals). Platelets contained DNA from all
164 human chromosomes, with an enrichment for mitochondrial DNA ($\sim 59\%$ of DNA content).
165 This is consistent with the reported presence of ~ 5 mitochondria per platelet²¹, and suggests
166 that each platelet contains ~ 56 kb of genomic DNA, in accordance with the previous estimate
167 of $\sim 0.1\%$ of the megakaryocyte genome present in platelets on average (given a mean
168 megakaryocyte ploidy of $12N^{22}$ and ~ 1000 platelets produced per megakaryocyte²³) (**Figure**
169 **3A**). We then focused on regions of the genome uniquely unmethylated in different
170 hematopoietic cell types as well as other cell types which contribute DNA to cfDNA such as
171 endothelial cells and hepatocytes, and evaluated the methylation of these regions in platelet
172 DNA. Importantly, only the megakaryocyte-unmethylated regions were unmethylated in
173 platelets (**Figure 3B-C**). Deconvolution analysis of the DNA methylation profile of platelet
174 DNA further identified megakaryocytes as the major contributors to platelet DNA (**Figure 3D**).

175
176

177 **The origins of MK-derived cfDNA**

178 After establishing that megakaryocyte-derived DNA is present in plasma, as well as in
179 platelets, we aimed to determine whether megakaryocyte-derived cfDNA originates directly
180 from megakaryocytes, or alternatively from platelets (either whole platelets that make their
181 way to cfDNA preps, or platelets that release cfDNA). To this end, we obtained plasma samples
182 from females who had received a transfusion of platelets from male donors (n=5). We reasoned
183 that if megakaryocyte cfDNA is derived from platelets, the cfDNA of recipients should contain
184 a large proportion of DNA containing the Y-chromosome. Interestingly, Y-chromosome
185 derived DNA could not be detected in these plasma samples more than 24 hours post-
186 transfusion, even though the half-life of transfused platelets is generally >2 days²⁴ (**Figure 4**
187 **and Supplementary Figure S7**). These findings suggest that megakaryocyte plasma cfDNA
188 is not derived from DNA found in platelets, but rather directly from megakaryocytes.

189
190

191 **A survey of megakaryocyte and erythroblast cfDNA in relevant diseases**

192 After establishing that circulating megakaryocyte DNA originates from megakaryocytes and
193 not from platelets, we reasoned that its concentration in plasma may be reflective of
194 megakaryocyte activity and turnover and hypothesized that megakaryocyte cfDNA would
195 increase in cases of hyperproliferation of megakaryocytes and decrease in cases of
196 hypoproliferation. To test this hypothesis, we collected samples from healthy individuals
197 (n=77), from patients with low platelet counts associated with hypoproliferation of
198 megakaryocytes due to chemotherapy treatment (n=5) and from patients with low platelet
199 counts associated with hyperproliferative megakaryocytes due to peripheral destruction of
200 platelets (Immune Thrombocytopenia [ITP]) (n=5). We also collected plasma from patients
201 with high platelet counts due to hyperproliferation of megakaryocytes (Essential
202 Thrombocythemia [ET]) (n=5). Healthy individuals had on average 510 genome equivalents

203 of megakaryocyte cfDNA/ml plasma (GE/ml) (**Table 1**, results detailed in **Supplementary**
204 **Tables S3, S4**). ET patients had significantly elevated levels of megakaryocyte cfDNA
205 (average 4242 GE/ml, $p < 0.05$). Interestingly, while patients with a hypoproliferative bone
206 marrow and patients with ITP had similar platelets counts, ITP patients had elevated
207 concentrations of circulating megakaryocyte DNA (average 1608 GE/ml, $p < 0.05$) while
208 patients with hypoproliferative bone marrows had reduced concentrations of circulating
209 megakaryocyte DNA (average 250 GE/ml, $p < 0.05$). These findings are consistent with
210 megakaryocyte cfDNA levels being reflective of megakaryocyte function and turnover (**Figure**
211 **5A-B**). Notably, erythroblast cfDNA was not reflective of megakaryocyte-platelet pathologies
212 but was significantly elevated in the plasma of patients with thalassemia major, a disease
213 involving increased, albeit ineffective, production of erythrocytes within the bone marrow
214 (average of 1658 erythroblast GE/ml, $p < 0.05$) (**Figure 5-C**). These findings confirm the
215 specificity of our targeted markers and support their potential utility in highly specific
216 identification of altered turnover of the respective cell types of origin.

217
218

219 **DISCUSSION**

220

221 In this work, we demonstrated that megakaryocytes are major contributors to plasma cfDNA
222 in healthy individuals, giving rise to ~26% of total cfDNA. In contrast, erythroblasts give rise
223 to a small but distinct proportion (~0.5-4%) of cfDNA in healthy individuals. These findings
224 contrast with previous reports that identified a major contribution of erythroblasts to cfDNA of
225 healthy individuals. One of these studies, from our own group, relied on a tissue methylome
226 atlas (based on Illumina methylation arrays) which contained the methylome of common
227 megakaryocyte-erythrocyte progenitor cells but not the megakaryocyte methylome¹². Another
228 study has demonstrated that genomic loci uniquely unmethylated in erythroblasts are also
229 partially unmethylated in plasma, concluding that erythroid cells are a major source of cfDNA
230 in healthy people¹³. A close examination of the methylation status of these marker loci revealed
231 that they are in fact unmethylated not only in erythroblasts but also in megakaryocytes
232 (**Supplementary Figure S8**). Thus, these markers are not sufficient to distinguish between
233 erythroid and megakaryocyte contributions to plasma, and the presence of unmethylated DNA
234 from these loci in healthy plasma is in fact consistent with a significant presence of
235 megakaryocyte DNA in circulation, in line with our current findings and as suggested by
236 analysis of histone modifications in circulating chromatin¹¹.

237 Megakaryocytes and erythroblasts have distinct mechanisms of cfDNA release.
238 Megakaryocytes are thought to undergo apoptosis during or immediately subsequent to
239 thrombopoiesis²⁵. Our analysis indicates that while a small proportion of the megakaryocyte
240 genome (~0.1%) is trapped within platelets, a fraction is fragmented to nucleosome-size pieces
241 and released to circulation as cfDNA. As for erythroblasts, the process of nuclear extrusion in
242 the final differentiation step of erythrocytes involves efficient removal by local macrophages²⁶.
243 Indeed, while 214 billion erythroblast nuclei are extruded every day²⁷, only a small amount of
244 erythroblast DNA is present in plasma. More experiments are needed to define the exact origin
245 of erythroblast cfDNA.

246

247 Additionally, we demonstrated that megakaryocyte- and erythroblast-specific cfDNA
248 concentration is reflective of megakaryocyte and red blood cell precursor activity; thus, it can
249 serve as a biomarker for diseases involving aberrant activity of these blood lineages, not
250 necessarily reflected in peripheral platelet and RBC counts.

251 Thrombocytopenia in cancer patients can be induced by chemotherapy, bone marrow
252 involvement or peripheral destruction of platelets as a result of immune processes.

253 Prolonged thrombocytopenia in cancer patients during therapy can be a diagnostic challenge.
254 Bone marrow biopsy is used for differential diagnosis, but the biopsy may be only partially
255 representative. Determining the cause of the thrombocytopenia is crucial, as treatment for such
256 thrombocytopenic patients will differ according to the pathogenesis of the thrombocytopenia.
257 Combined with peripheral blood smear and bone marrow biopsy, cfDNA measurements can
258 potentially distinguish between these clinical scenarios and guide treatment decisions.
259 ITP is a syndrome characterized by antibody-mediated platelet destruction and variably
260 reduced platelet production²⁸. Bone marrow biopsies of ITP patients show normal or increased
261 numbers of megakaryocytes. There is currently no diagnostic tool for ITP. We demonstrated
262 that megakaryocyte cfDNA is elevated in ITP. More experiments are needed in ITP patients
263 and healthy controls to determine whether megakaryocyte methylation biomarkers can serve
264 as a diagnostic tool for ITP.

265
266 This study also provides the first evidence that platelets contain megakaryocyte-derived
267 nuclear DNA. An important implication of this situation is that it provides a non-invasive
268 window into the genome and epigenome of the megakaryocyte, a cell type particularly difficult
269 to interrogate due to its relative scarceness within the bone marrow. The presence of somatic
270 mutations in megakaryocytes, as well as epigenomic aberrations, can therefore be interrogated
271 by analysis of platelet samples. Additionally, gene expression of the megakaryocyte, as
272 reflected by transcription related epigenetic modifications, may be indirectly evaluated via the
273 platelet epigenome.

274 We have not addressed whether platelet DNA is concentrated in a subset of platelets or if it is
275 distributed randomly throughout the platelet population. Additionally, the fate and function of
276 the megakaryocyte genomic fragments trapped within platelets is not clear. It is well
277 established that platelets contain RNA which undergoes translation to protein, yet this RNA is
278 generally understood to have been transcribed in the megakaryocyte prior to platelet formation
279 or from mitochondrial DNA within the platelet²⁹. Given our findings that platelets contain
280 nuclear DNA, the question as to whether transcription of nuclear DNA occurs within the
281 platelet should be revisited.

282

283

284 **MATERIALS AND METHODS**

285

286 **Platelet isolation**

287 Platelets were isolated from donors via single donor plateletpheresis for the purpose of platelet
288 transfusion at the Hadassah Medical Center Blood Bank. Platelets which had not been
289 transfused within one week were obtained for research purposes. In order to subsequently
290 purify platelets from surrounding plasma, the platelets were diluted in PBS noCa²⁺ & Mg²⁺ or
291 tyrode's buffer (1/3 SDP+2/3 PBS). Platelet activation was inhibited with citric acid (5ul of 1M
292 citric acid per 1ml or 10% citrate from collection tubes). Subsequently, centrifugation was
293 performed at 750g (3000rpm) for 8 minutes at room temperature. A platelet pellet was obtained
294 which was diluted in PBS with citric acid (5 ul citric acid/ml PBS). Optionally, Dnase I was
295 added at a concentration of 100µg/ml and samples were incubated for 20 minutes in a heatbath
296 at 37 degrees Celsius. Samples were then centrifuged again at 750g for 8 min and then pellets
297 were suspended in 1.4 ml PBS (no citrate).

298

299 **Subject enrollment**

300 This study was conducted according to protocols approved by the Institutional Review Board
301 at the study site, with procedures performed in accordance with the Declaration of Helsinki.
302 Blood samples were obtained from donors who have provided written informed consent.

303 Subject characteristics are presented in Supplementary Table S3 and in Supplementary Table
304 S4. Patients were recruited with acute ITP, with less than 35000 platelets/ul (n=5), with
305 Essential Thrombocytopenia (n=5, >500000 platelets/ul); 5 patients with Acute Myeloid
306 Leukemia (AML), 14 days after the start of induction chemotherapy with cytarabine and
307 daunorubicin (7+3 regimen) were recruited as patients with hypoplastic bone marrow.
308 Additionally, 3 patients were recruited with thalassemia major. 77 healthy controls were
309 recruited. Healthy controls were excluded if platelet count was less than 150000 platelets/ul
310 or greater than 500000 platelets/ul.

311

312 **Blood sample collection and processing**

313 Blood samples were collected by routine venipuncture in 10 ml EDTA Vacutainer tubes or
314 Streck blood collection tubes and stored at room temperature for up to 4 hr or 5 days,
315 respectively. Tubes were centrifuged at 1500× g for 10 min at 4°C (EDTA tubes) or at room
316 temperature (Streck tubes). The supernatant was transferred to a fresh 15 ml conical tube
317 without disturbing the cellular layer and centrifuged again for 10 min at 3000× g. The
318 supernatant was collected and stored at -80°C. cfDNA was extracted from 2 to 4 ml of
319 plasma using the QIASymphony liquid handling robot (Qiagen). cfDNA concentration was
320 determined using Qubit double-strand molecular probes kit (Invitrogen) according to the
321 manufacturer's instructions.

322 DNA derived from all samples was treated with bisulfite using EZ DNA Methylation-Gold
323 (Zymo Research), according to the manufacturer's instructions, and eluted in 24 µl elution
324 buffer.

325

326 **Whole-genome bisulfite sequencing of reference cell types**

327 Previously published single-cell genome-wide methylation profiles of megakaryocytes and
328 genome-wide profiles of megakaryocyte-erythrocyte progenitors³⁰ of three individuals were
329 obtained from Blueprint Epigenome. Single-cell methylation profiles were grouped by
330 individual for further analysis.

331 Erythroblasts were isolated as follows: Bone marrow was diluted with 3 equivalent volumes
332 of PBS, filtered through a 100µm cell strainer and laid over Lymphoprep density gradient
333 medium (Stemcell Technologies). After centrifugation, interphase bone marrow mononuclear
334 cells were transferred to PBS, washed and red blood cells (RBC) were lysed using standard
335 RBC lysis buffer.

336 CD45-negative, CD235a and CD71-positive erythrocyte precursors were FACS-sorted on a
337 BD FACSAria™ III flow cytometer.

338 Granulocytes, monocytes, B cells, NK cells, CD3+ T cells, CD4+ T cells, CD8+ T cells,
339 hepatocytes and endothelial cells were isolated as previously described³¹.

340 Up to 75 ng of sheared gDNA was subjected to bisulfite conversion using the EZ-96 DNA
341 Methylation Kit (Zymo Research; Irvine, CA), with liquid handling on a Hamilton MicroLab
342 STAR (Hamilton; Reno, NV). Dual indexed sequencing libraries were prepared using Accel-
343 NGS Methyl-Seq DNA library preparation kits (Swift BioSciences; Ann Arbor, MI) and
344 custom liquid handling scripts executed on the Hamilton MicroLab STAR. Libraries were
345 quantified using KAPA Library Quantification Kits for Illumina Platforms (Kapa
346 Biosystems; Wilmington, MA). Four uniquely dual indexed libraries, along with 10% PhiX
347 v3 library (Illumina; San Diego, CA), were pooled and clustered on a Illumina NovaSeq 6000
348 S2 flow cell followed by 150-bp paired-end sequencing.

349

350 **Selection of megakaryocyte and erythroblast methylation markers**

351 CpGs were identified as being cell type specific if they were unmethylated (<20%
352 methylation) in all samples of the cell type of interest and methylated in all other samples

353 (>80% methylation) or if they were methylated in all samples of the cell type of interest and
354 unmethylated in other samples.

355 For selection of markers for analysis by targeted bisulfite sequencing, CpGs with neighboring
356 CpGs which were also cell type specific and located in a CpG dense genomic region (≥ 5
357 CpGs within 120 bp) were selected for further analysis. DNA methylation of candidate
358 regions were then compared to DNA methylation at these regions in genome-wide
359 methylation profiles of multiple tissues published as part of Roadmap Epigenomics, using the
360 same criteria as described above.

361 Genome coordinates of cell-type specific methylation markers and primer sequences are
362 included in **Supplementary Table S1**.

363

364 **PCR**

365 To efficiently amplify and sequence multiple targets from bisulfite-treated cfDNA, we used a
366 two-step multiplexed PCR protocol, as described³². In the first step, up to 10 primer pairs
367 were used in one PCR reaction to amplify regions of interest from bisulfite-treated DNA,
368 independent of methylation status. Primers were 18–30 base pairs (bp) with primer melting
369 temperature ranging from 58°C to 62°C. To maximize amplification efficiency and minimize
370 primer interference, the primers were designed with additional 25 bp adaptors comprising
371 Illumina TruSeq Universal Adaptors without index tags. All primers were mixed in the same
372 reaction tube. For each sample, the PCR was prepared using the QIAGEN Multiplex PCR Kit
373 according to manufacturer's instructions with 7 μ l of bisulfite-treated cfDNA. Reaction
374 conditions for the first round of PCR were: 95°C for 15 min, followed by 30 cycles of 95°C
375 for 30 s, 57°C for 3 min and 72°C for 1.5 min, followed by 10 min at 68°C.

376 In the second PCR step, the products of the first PCR were treated with Exonuclease I
377 (ThermoScientific) for primer removal according to the manufacturer's instructions. Cleaned
378 PCR products were amplified using one unique TruSeq Universal Adaptor primer pair per
379 sample to add a unique index barcode to enable sample pooling for multiplex Illumina
380 sequencing. The PCR was prepared using 2 \times PCR BIO HS Taq Mix Red Kit (PCR
381 Biosystems) according to manufacturer's instructions. Reaction conditions for the second
382 round of PCR were: 95°C for 2 min, followed by 15 cycles of 95°C for 30 s, 59°C for 1.5
383 min, 72°C for 30 s, followed by 10 min at 72°C. The PCR products were then pooled, run on
384 3% agarose gels with ethidium bromide staining, and extracted by Zymo GEL Recovery kit.

385

386 **NGS and analysis of PCR products**

387 Pooled PCR products were subjected to multiplex NGS using the *NextSeq* 500/550 v2
388 Reagent Kit (Illumina). Sequenced reads were separated by barcode, and aligned to the target
389 sequence with Bismark, using a computational pipeline available

390 (<https://github.com/Joshmoss11/btseq>). CpGs were considered methylated if 'CG' was read
391 and unmethylated if 'TG' was read. Proper bisulfite conversion was assessed by analyzing
392 methylation of non-CpG cytosines. We then determined the fraction of molecules in which
393 all CpG sites were unmethylated. The fraction obtained was multiplied by the concentration
394 of cfDNA measured in each sample, to obtain the concentration of tissue-specific cfDNA
395 from each donor. Given that the mass of a haploid human genome is 3.3 pg, the concentration
396 of cfDNA could be converted from units of ng/ml to haploid GE/ml by multiplying by a
397 factor of 303.

398 Sequenced molecules were considered to be unmethylated (for specifically unmethylated
399 markers) if all CpGs on the sequenced DNA fragment were unmethylated. The fraction of
400 DNA derived from the cell type of interest for each marker (for specifically unmethylated
401 markers) was calculated as the fraction of completely unmethylated molecules among all
402 sequenced molecules from the marker region.

403

404 **Whole-genome bisulfite sequencing of platelet DNA**

405 DNA was extracted from three platelet samples using the QIASymphony liquid handling
406 robot (Qiagen). Subsequently, whole-genome bisulfite sequencing libraries were generated
407 with Swift AccelNGS Methyl-Seq
408 DNA Library preparation protocol (Swift Biosciences, Ann Arbor, MI). Paired-end
409 sequencing was performed on the Illumina Nextseq 550 System of 300 bp per read at an
410 average depth of 2.54x.

411

412 **Whole-genome bisulfite sequencing computational processing and analysis**

413 Paired-end FASTQ files were mapped to the human (hg19) genome using bwa-meth (V
414 0.2.0), with default parameters³³, then converted to BAM files using SAMtools (V 1.9)³⁴.
415 Duplicated reads were marked by Sambamba (V 0.6.5), with parameters “-l 1 -t 16 --sort-
416 buffer-size 16000 --overflow-list-size 10000000”³⁵.
417 Reads with low mapping quality, duplicated, or not mapped in a proper pair were excluded
418 using SAMtools view with parameters -F 1796 -q 10.
419 Reads were stripped from non-CpG nucleotides and converted to BETA files using wgbstools
420 (V 0.1.0) (https://github.com/nloyfer/wgbs_tools)³¹.
421 For comparison of platelet DNA methylation to DNA methylation of other cell types, bone
422 marrow-residing immune cell progenitor cells were obtained from Blueprint Epigenome³⁶.
423 genome-wide methylation profiles of methylation profiles of hepatocytes, endothelial cells
424 and immune cells, which have been found to release DNA to plasma under normal
425 conditions¹², were obtained as described³¹. Regions with methylation unique to each cell type
426 were identified by segmenting the genome into multi-sample homogenous blocks as
427 previously described³¹, and identifying regions unmethylated (<20%) or methylated (>80%)
428 in a specific cell type. Deconvolution of the platelet DNA methylation profiles at the resultant
429 regions was performed by NNLS as previously described¹².

430

431 **Statistics**

432 To determine the significance of differences between groups we used a non-parametric two-
433 tailed Mann-Whitney test. P-values were considered significant at < 0.05. Samples that were
434 detected as outliers were excluded. All statistical analyses were performed with R (version
435 4.1)³⁷.

436

437 **List of Supplementary Materials**

438 Fig S1 to S8

439 Tables S1 to S4

440

441 **References**

- 442 1. Lo, Y. M. D. *et al.* Maternal plasma DNA sequencing reveals the genome-wide
443 genetic and mutational profile of the fetus. *Sci. Transl. Med.* (2010).
444 doi:10.1126/scitranslmed.3001720
- 445 2. De Vlaminck, I. *et al.* Circulating cell-free DNA enables noninvasive diagnosis of
446 heart transplant rejection. *Sci. Transl. Med.* (2014). doi:10.1126/scitranslmed.3007803
- 447 3. Wan, J. C. M. *et al.* Liquid biopsies come of age: Towards implementation of
448 circulating tumour DNA. *Nature Reviews Cancer* **17**, 223–238 (2017).
- 449 4. Dor, Y. & Cedar, H. Principles of DNA methylation and their implications for biology
450 and medicine. *Lancet* (2018). doi:10.1016/S0140-6736(18)31268-6
- 451 5. Zemmour, H. *et al.* Non-invasive detection of human cardiomyocyte death using

- 452 methylation patterns of circulating DNA. *Nat. Commun.* (2018). doi:10.1038/s41467-
453 018-03961-y
- 454 6. Lehmann-Werman, R. *et al.* Monitoring liver damage using hepatocyte-specific
455 methylation markers in cell-free circulating DNA. *JCI Insight* (2018).
456 doi:10.1172/jci.insight.120687
- 457 7. Lehmann-Werman, R. *et al.* Identification of tissue-specific cell death using
458 methylation patterns of circulating DNA. *Proc. Natl. Acad. Sci. U. S. A.* **113**, E1826–
459 E1834 (2016).
- 460 8. Liu, M. C. *et al.* Sensitive and specific multi-cancer detection and localization using
461 methylation signatures in cell-free DNA. *Ann. Oncol.* (2020).
462 doi:10.1016/j.annonc.2020.02.011
- 463 9. Snyder, M. W., Kircher, M., Hill, A. J., Daza, R. M. & Shendure, J. Cell-free DNA
464 Comprises an In Vivo Nucleosome Footprint that Informs Its Tissues-Of-Origin. *Cell*
465 **164**, 57–68 (2016).
- 466 10. Lo, Y. M. D., Han, D. S. C., Jiang, P. & Chiu, R. W. K. Epigenetics, fragmentomics,
467 and topology of cell-free DNA in liquid biopsies. *Science (80-)*. **372**, (2021).
- 468 11. Sadeh, R. *et al.* ChIP-seq of plasma cell-free nucleosomes identifies cell-of-origin
469 gene expression programs. *bioRxiv* (2019). doi:10.1101/638643
- 470 12. Moss, J. *et al.* Comprehensive human cell-type methylation atlas reveals origins of
471 circulating cell-free DNA in health and disease. *Nat. Commun.* **9**, 5068 (2018).
- 472 13. Lam, W. K. J. *et al.* DNA of Erythroid Origin Is Present in Human Plasma and
473 Informs the Types of Anemia. *Clin. Chem.* **63**, 1614–1623 (2017).
- 474 14. Shearstone, J. R. *et al.* Global DNA Demethylation During Erythropoiesis in vivo.
475 *Science* **334**, 799 (2011).
- 476 15. Schulz, V. P. *et al.* A Unique Epigenomic Landscape Defines Human Erythropoiesis.
477 *Cell Rep.* **28**, 2996-3009.e7 (2019).
- 478 16. Fox-Fisher, I. *et al.* Remote immune processes revealed by immune-derived
479 circulating cell-free dna. *Elife* **10**, (2021).
- 480 17. Bray, P. F. *et al.* The complex transcriptional landscape of the anucleate human
481 platelet. *BMC Genomics* **14**, 1–15 (2013).
- 482 18. Frydman, G. H. *et al.* Megakaryocytes contain extranuclear histones and may be a
483 source of platelet-associated histones during sepsis. *Sci. Rep.* (2020).
484 doi:10.1038/s41598-020-61309-3
- 485 19. Nilsson, R. J. A. *et al.* Blood platelets contain tumor-derived RNA biomarkers. *Blood*
486 **118**, 3680–3683 (2011).
- 487 20. In 't Veld, S. G. J. G. *et al.* Detection and localization of early- and late-stage cancers
488 using platelet RNA. *Cancer Cell* **40**, 999-1009.e6 (2022).
- 489 21. Shuster, R. C., Rubenstein, A. J. & Wallace, D. C. Mitochondrial DNA in anucleate
490 human blood cells. *Biochem. Biophys. Res. Commun.* **155**, 1360–1365 (1988).
- 491 22. Bessman, J. D. The relation of megakaryocyte ploidy to platelet volume. *Am. J.*
492 *Hematol.* **16**, 161–170 (1984).
- 493 23. Zadehkoochak, M. *et al.* Clinical Physics and Physiological Measurement Analysis of
494 the sensitivity method of reconstruction using spectral expansion Platelet
495 thermophysiology: a new field of investigation dependent upon an improved sub-

- 496 ambient platelet aggregometer The origin Of platelet count and volume. *Clin. Phys.*
497 *Physiol. Meas* **5**, 145 (1984).
- 498 24. Cesar, J. M., Vecino, A. M., Jesu', J. & Cesar, J. M. Survival and function of
499 transfused platelets. Studies in two patients with congenital deficiencies of platelet
500 membrane glycoproteins. <https://doi.org/10.1080/09537100902751925> **20**, 158–162
501 (2009).
- 502 25. McArthur, K., Chappaz, S. & Kile, B. T. Apoptosis in megakaryocytes and platelets:
503 the life and death of a lineage. *Blood* **131**, 605–610 (2018).
- 504 26. Chasis, J. A. & Mohandas, N. Erythroblastic islands: niches for erythropoiesis. *Blood*
505 **112**, 470–478 (2008).
- 506 27. Sender, R. & Milo, R. Brief CommuniCation The distribution of cellular turnover in
507 the human body. *Nat. Med.* **27**, 45–48 (2021).
- 508 28. Cines, D. B., Cuker, A. & Semple, J. W. Pathogenesis of immune thrombocytopenia.
509 *Presse Med.* **43**, e49–e59 (2014).
- 510 29. Schubert, S., Weyrich, A. S. & Rowley, J. W. A tour through the transcriptional
511 landscape of platelets. *Blood* **124**, 493–502 (2014).
- 512 30. Farlik, M. *et al.* DNA Methylation Dynamics of Human Hematopoietic Stem Cell
513 Differentiation. *Cell Stem Cell* (2016). doi:10.1016/j.stem.2016.10.019
- 514 31. Loyfer, N. *et al.* A human DNA methylation atlas reveals principles of cell type-
515 specific methylation and identifies thousands of cell type-specific regulatory elements.
516 *bioRxiv* 2022.01.24.477547 (2022). doi:10.1101/2022.01.24.477547
- 517 32. Neiman, D. *et al.* Multiplexing DNA methylation markers to detect circulating cell-
518 free DNA derived from human pancreatic β cells. *JCI Insight* **5**, (2020).
- 519 33. Pedersen, B. S., Eyring, K., De, S., Yang, I. V & Schwartz, D. A. Fast and accurate
520 alignment of long bisulfite-seq reads. (2014).
- 521 34. Li, H. *et al.* The Sequence Alignment/Map format and SAMtools. *Bioinformatics* **25**,
522 2078–2079 (2009).
- 523 35. Tarasov, A., Vilella, A. J., Cuppen, E., Nijman, I. J. & Prins, P. Sambamba: fast
524 processing of NGS alignment formats. *Bioinformatics* **31**, 2032–2034 (2015).
- 525 36. Adams, D. *et al.* BLUEPRINT to decode the epigenetic signature written in blood.
526 *Nat. Biotechnol.* 2012 303 **30**, 224–226 (2012).
- 527 37. R Core Team. R: A Language and Environment for Statistical Computing. (2018).

528

529 **Acknowledgments**

530 We acknowledge the donors of the biological samples presented in this study for their
531 benevolent contribution to science. We thank Dr. Abed Nasereddin and Dr. Idit Shiff of the
532 Core Research Facility of the Faculty of Medicine of the Hebrew University of Jerusalem for
533 performing the targeted bisulfite sequencing experiments and WGBS of platelets presented in
534 the article, and the blood bank of the Hadassah Medical Center for aid in obtaining platelet
535 samples. We thank Prof. Neta Goldschmidt for recruiting patients to the study.

536

537 **Funding**

538 This study was supported by grants from The Ernest and Bonnie Beutler Research Program
539 of Excellence in Genomic Medicine (FREEDOME), The Helmsley Charitable Trust,

540 Alzheimer’s Drug Discover Foundation, a Merck Grant for Multiple Sclerosis Innovation
541 (GMSI), The Israel Science Foundation, the Waldholtz/Pakula family, and the Robert M. and
542 Marilyn Sternberg Family Charitable Foundation (to YD). YD holds the Walter and Greta
543 Stiel Chair and Research grant in Heart studies.

544

545 **Author contributions**

546 Conceptualization: JM, YD, RS, AA, RB
547 Methodology: JM, RB, YD, GC, BG, RS, AK, ES, YK
548 Investigation: JM, RB, AK, AA, ES
549 Visualization: JM, AK
550 Funding acquisition: YD
551 Project administration: YD, RS, AA, JM
552 Supervision: YD, RS, AA
553 Writing – original draft: JM
554 Writing – review & editing: JM, YD, BG, AA, YK, RB, GC, RS

555 **Competing interests**

556 JM, RS, BG, and YD are inventors of a patent filing describing analysis of platelet DNA as
557 well as megakaryocyte methylation markers and their use for cfDNA analysis. All remaining
558 authors have declared no conflicts of interest.

559

560 **Data and materials availability**

561 Results of targeted bisulfite sequencing for erythroblast and megakaryocyte methylation
562 markers are included in Supplementary Table S3.
563 Whole-genome bisulfite sequencing data of platelet DNA has been deposited at GEO,
564 accession number GSE206818.

565

566

567

568

569

570

571

572

573

574

575

576

577

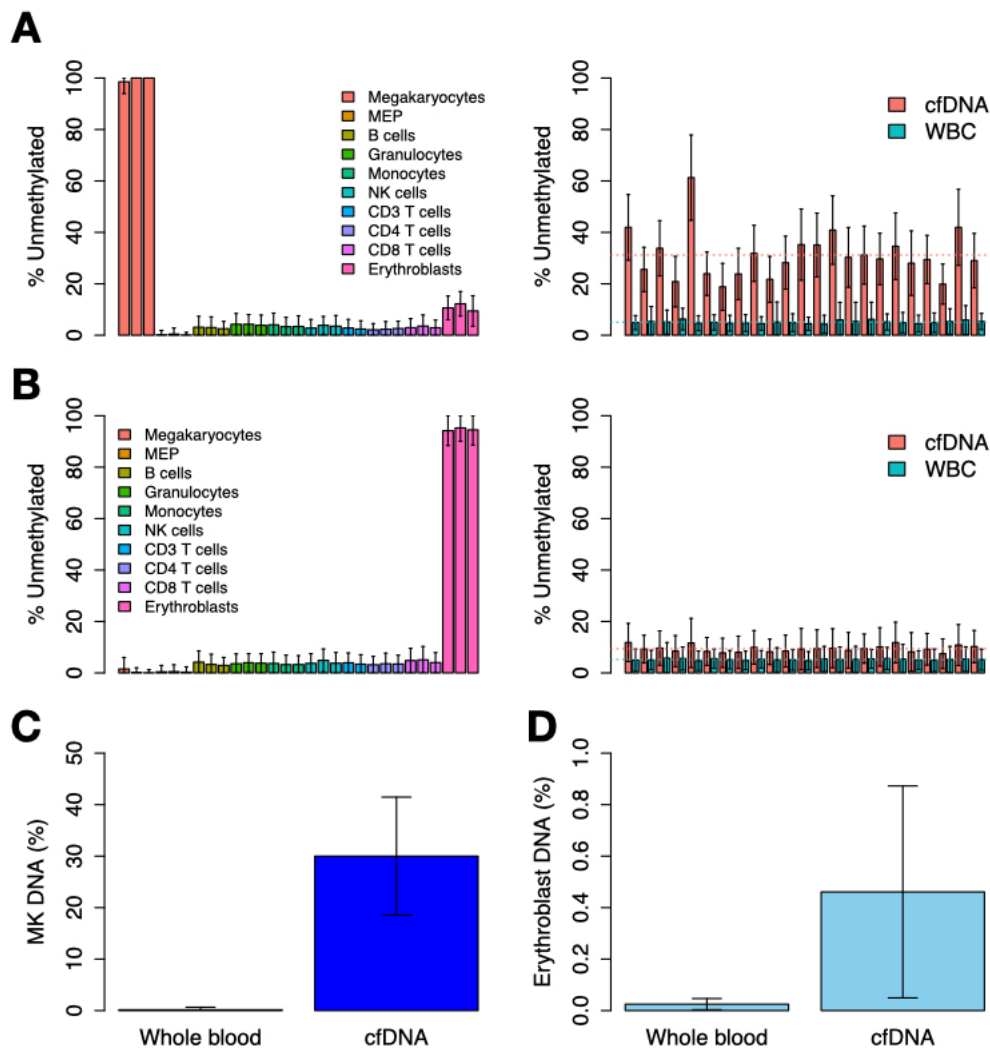
578

579

580

581

582



583

584

585

586

587

588

589

590

591

592

593

594

595

596

597

598

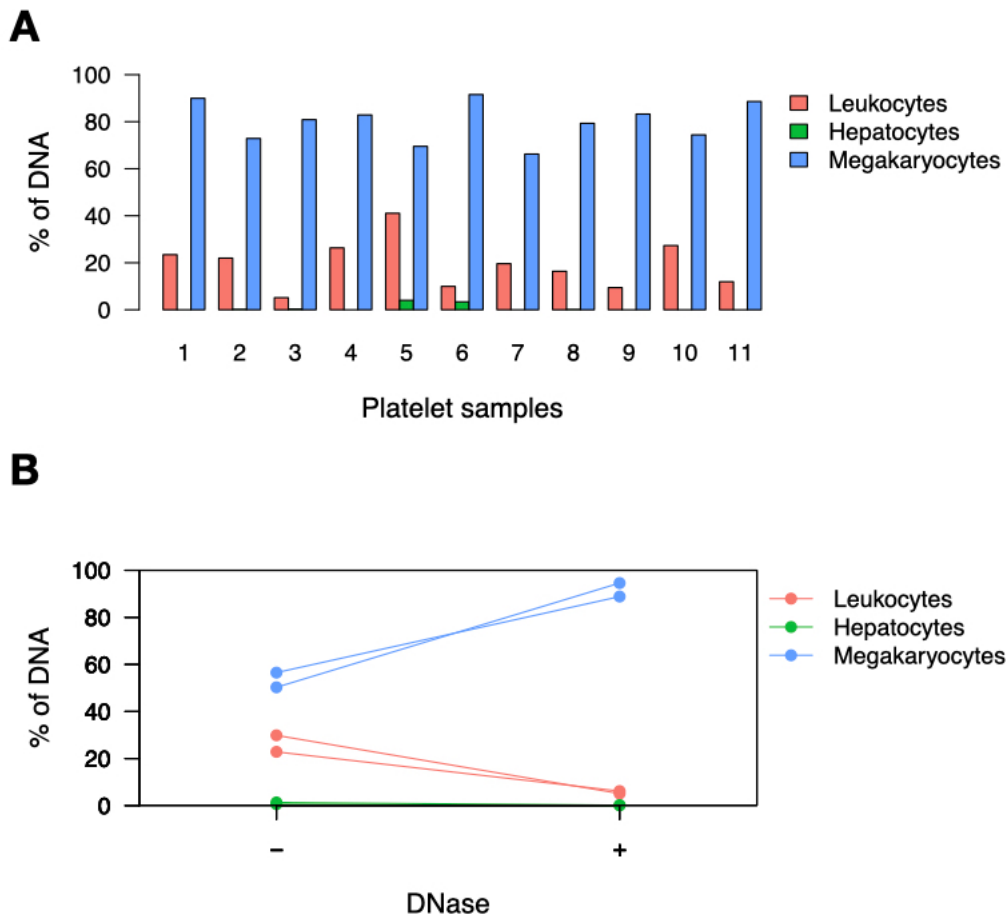
599

600

601

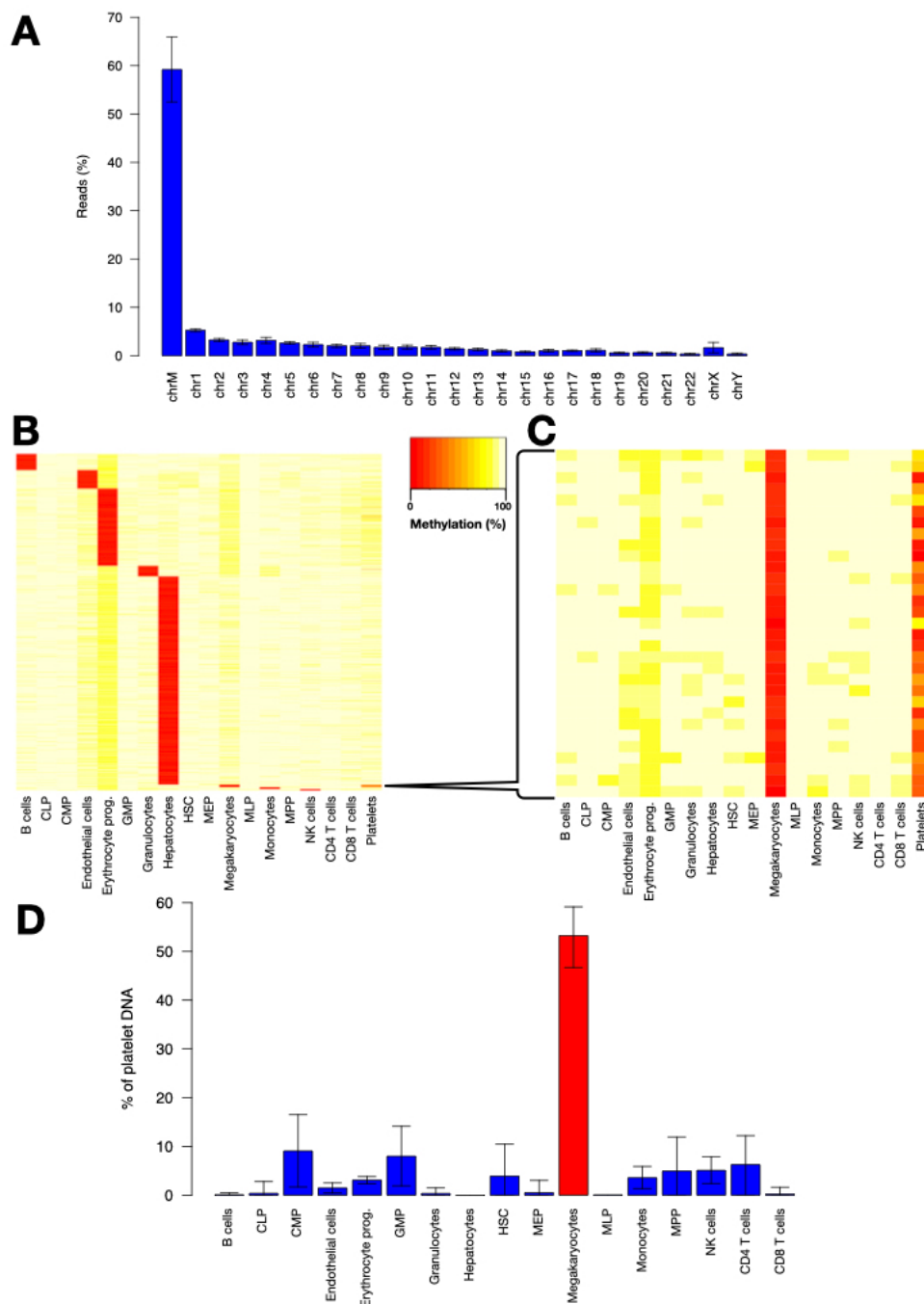
Fig. 1. Comparative analysis of erythroblast and megakaryocyte methylomes, and their representation in plasma. (A) Genomic loci unmethylated specifically in megakaryocytes (n=97 loci) were identified by comparison to other cell types of hematopoietic origin (left) and subsequently evaluated by WGBS of white blood cells (WBC) and cell-free DNA (cfDNA) of 23 individuals (right). These sites were, on average, 5% unmethylated in WBC and 31% unmethylated in cfDNA. For each individual, the sites were significantly hypomethylated in cfDNA ($p < 0.05$). Average percent of unmethylated sites is marked by a dotted line for cfDNA (red) and WBC (blue). (B) Genomic loci unmethylated specifically in erythroblasts (n=1884 loci) were identified by comparison to other cell types of hematopoietic origin (left) and subsequently evaluated by WGBS of white blood cells (WBC) and cell-free DNA (cfDNA) of 23 individuals (right). These sites were, on average, 5% unmethylated in WBC and 9% unmethylated in cfDNA. For each individual, the sites were significantly hypomethylated in cfDNA ($p < 0.05$). Average percent of unmethylated sites is marked by a dotted line for cfDNA (red) and WBC (blue). (C) Targeted bisulfite-sequencing of megakaryocyte-specific unmethylated regions in whole blood (n=26) and cfDNA (n=62) of healthy individuals, demonstrating a higher percentage of megakaryocyte-derived DNA in cfDNA compared to WBC ($p < 0.05$). (D) Targeted bisulfite-sequencing of erythroblast-specific unmethylated regions in whole blood (n=15) and cfDNA (n=71) of healthy

602 individuals, demonstrating a higher percentage of erythroblast-derived DNA in cfDNA
603 compared to WBC ($p < 0.05$).



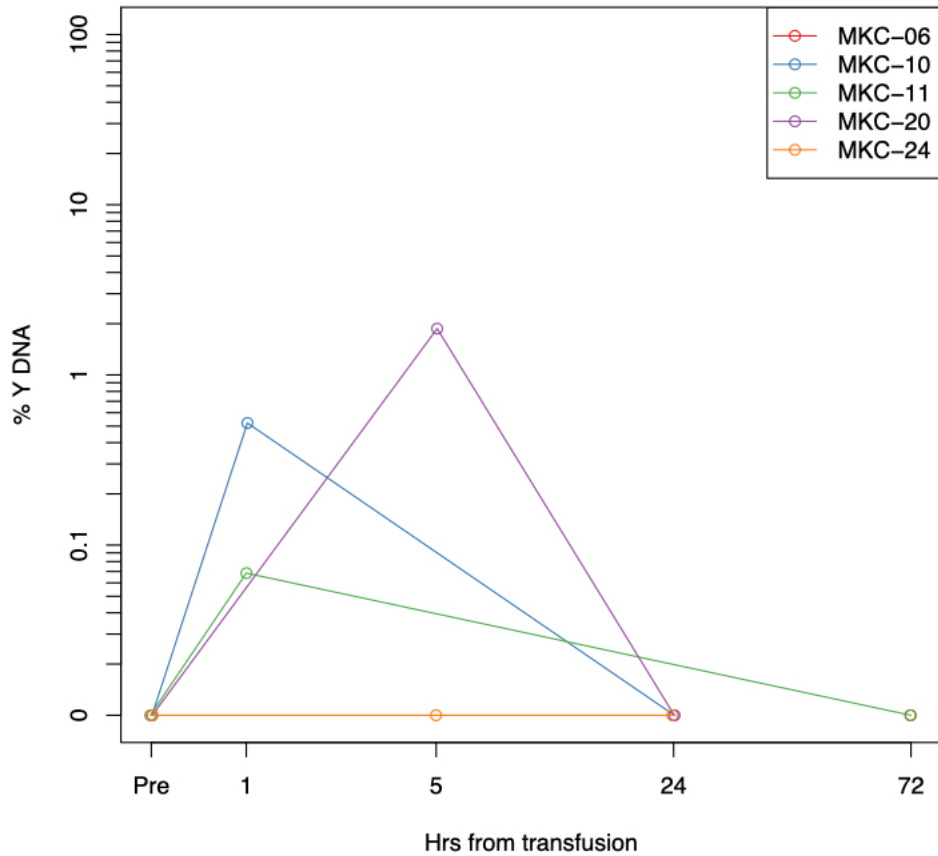
604

605 **Fig. 2. Platelets contain genomic DNA derived from megakaryocytes.** (A) DNA extracted from
606 platelet concentrates contains DNA derived from megakaryocytes, leukocytes and
607 hepatocytes, as measured by targeted bisulfite sequencing of cell-type specific unmethylated
608 genomic regions. (B) Uncentrifuged platelet concentrates (platelets in plasma) were analyzed
609 with or without DNase treatment, demonstrating that DNase treatment reduces leukocyte and
610 liver, but not MK markers in platelets.



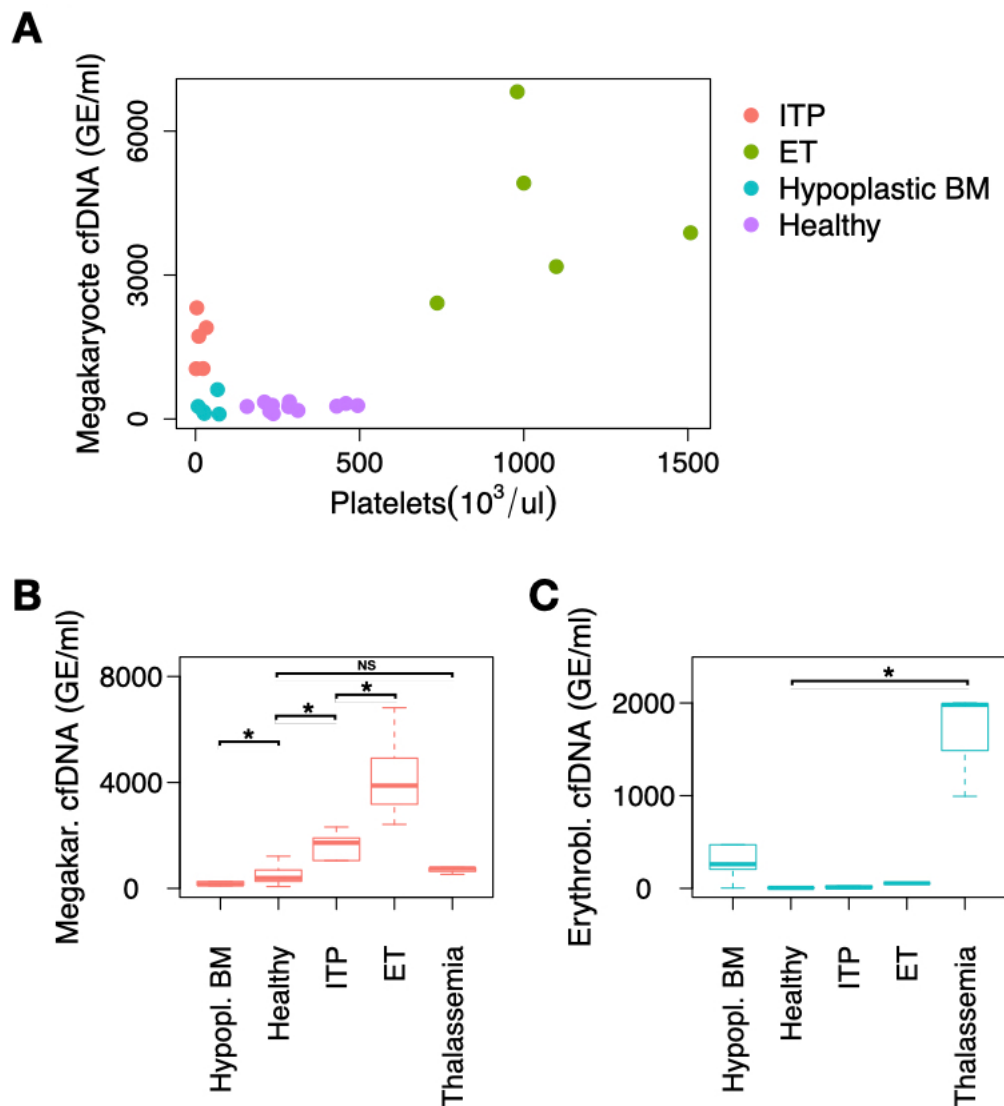
611

612 **Fig. 3. Genome-wide analysis of platelet DNA supports megakaryocyte origin.** (A) Platelet DNA
 613 is derived from all human chromosomes; however, the majority is mitochondrial DNA. The
 614 mean of three platelet samples is plotted with error bars representing standard deviations. (B-
 615 C) Regions uniquely unmethylated in cell types of hematopoietic origin, hepatocytes and
 616 endothelial cells were identified as described (Methods). Megakaryocyte-unique
 617 unmethylated regions are unmethylated in platelets as well. HSC – Hematopoietic stem cell,
 618 MPP – Multipotent progenitor, CMP – Common myeloid progenitor, CLP – Common
 619 lymphoid progenitor, MLP – Multi-lymphoid progenitor, GMP – Granulocyte macrophage
 620 progenitor, MEP – Megakaryocyte erythroid progenitor. (D) Deconvolution of platelet DNA
 621 methylation demonstrated megakaryocyte DNA as the main component of platelet DNA.
 622 Error bars represent 90% confidence intervals calculated by bootstrapping over 10000
 623 iterations.



624

625 **Fig. 4. Gender-mismatched platelet transfusions suggest that platelets are not the source of**
626 **megakaryocyte DNA.** The ratio of concentration of DNA from the SRY gene, located on the
627 Y-chromosome, to DNA from the Beta-actin gene, located on chromosome 7, was evaluated
628 in the plasma of female recipients of platelets from male donors, by massive parallel
629 sequencing. At 24-72 hours after transfusion there was no remaining male DNA detectable.



630

631 **Fig. 5. Targeted analysis of megakaryocyte (MK) and erythroblast methylation markers in**
632 **plasma samples. (A)** Genome equivalents (GE) per milliliter plasma of megakaryocyte DNA
633 in samples from healthy donors and patients with ITP, ET and hypoplastic bone marrow (after
634 chemotherapy). **(B)** MK DNA is present in significantly different concentrations between
635 healthy, ITP, ET and hypoplastic bone marrow ($p < 0.05$). MK DNA is not significantly
636 different in Thalassemia as compared to healthy individuals. **(C)** Erythroblast cfDNA is
637 significantly elevated in Thalassemia compared to healthy individuals, as well as compared to
638 ET ($p < 0.05$). * $p < 0.05$

639

640

641

642

643 **Table 1. Description and results of clinical samples analyzed for megakaryocyte and**
644 **erythroblast cfDNA concentrations.**

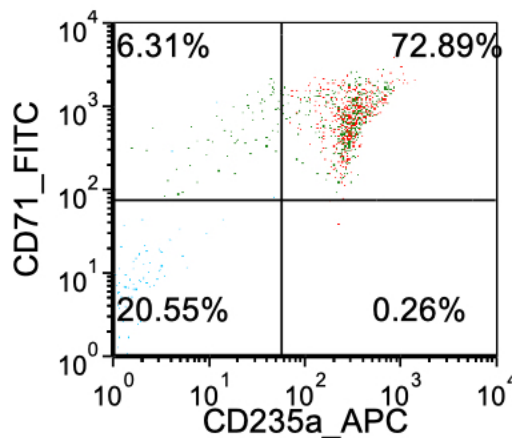
Group	Count	Age (avg.)	Age (SD)	Female (n)	Platelet count (n/ul)	Megakaryocyte cfDNA (avg. GE/ml)	Erythroblast cfDNA (avg. GE/ml)
ITP	5	42	25	3	14400	1608	21
ET	5	67	15	3	1064600	4242	112
Hypoplastic BM	5	60	21	2	39600	250	2126
Healthy	77	36	15	40	302545	510	7
Thalassemia	3	48	7	2	619667	690	1658

645

646

647 **Supplementary Figures**

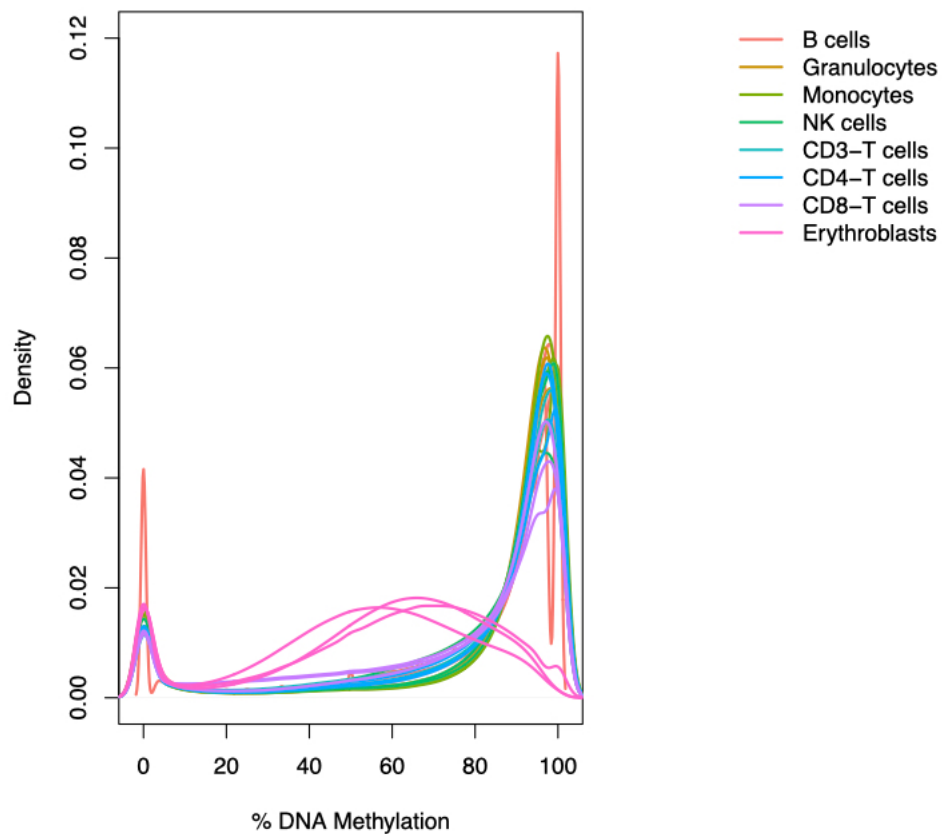
648



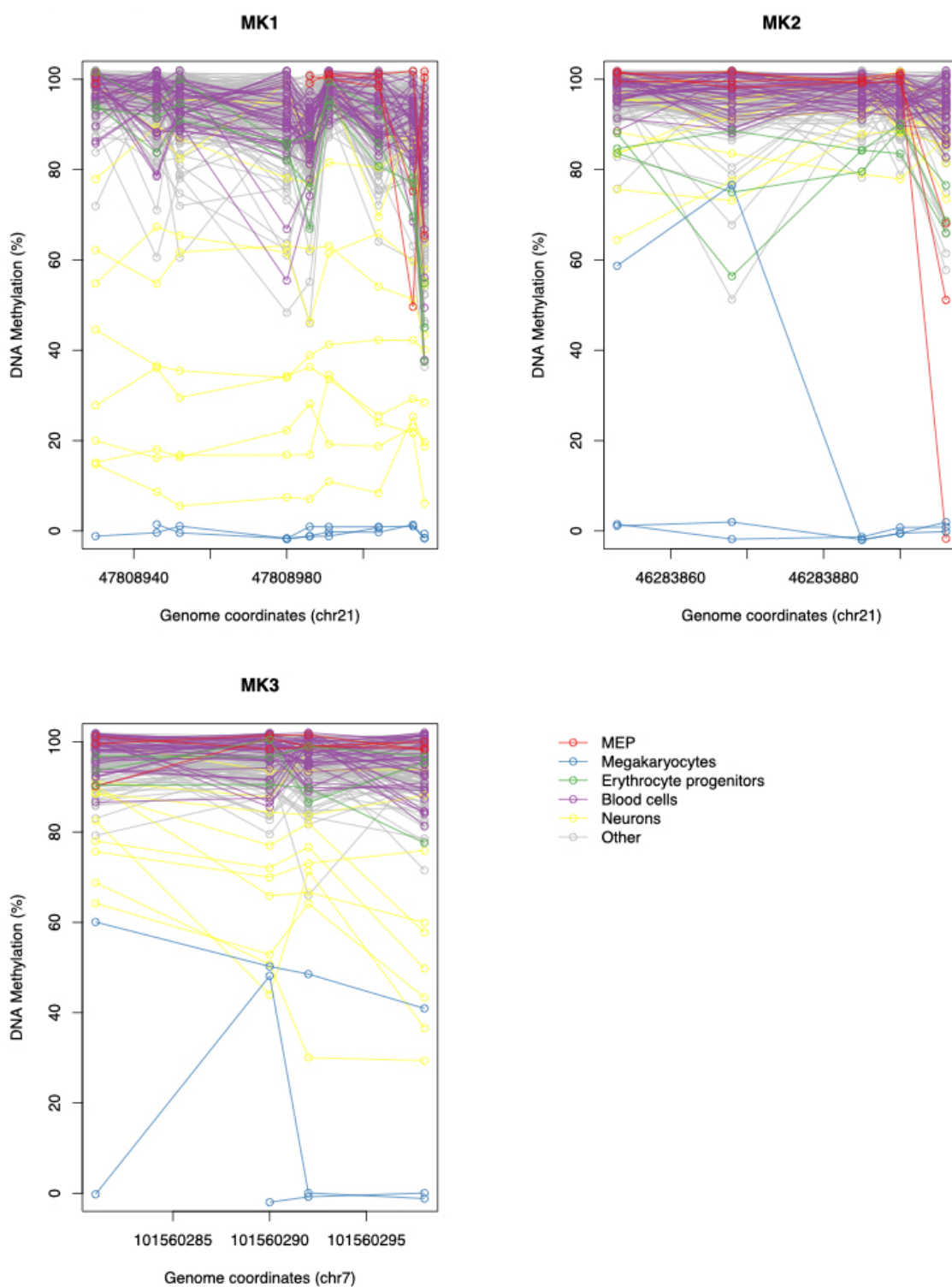
649

650 **Fig S1. FACS plot of erythroid cells sorted from bone marrow. CD45-negative, CD235a**
651 **and CD71-positive erythrocyte precursors, derived from bone marrow were FACS-sorted on a**
652 **BD FACSAria™ III flow cytometer.**

653

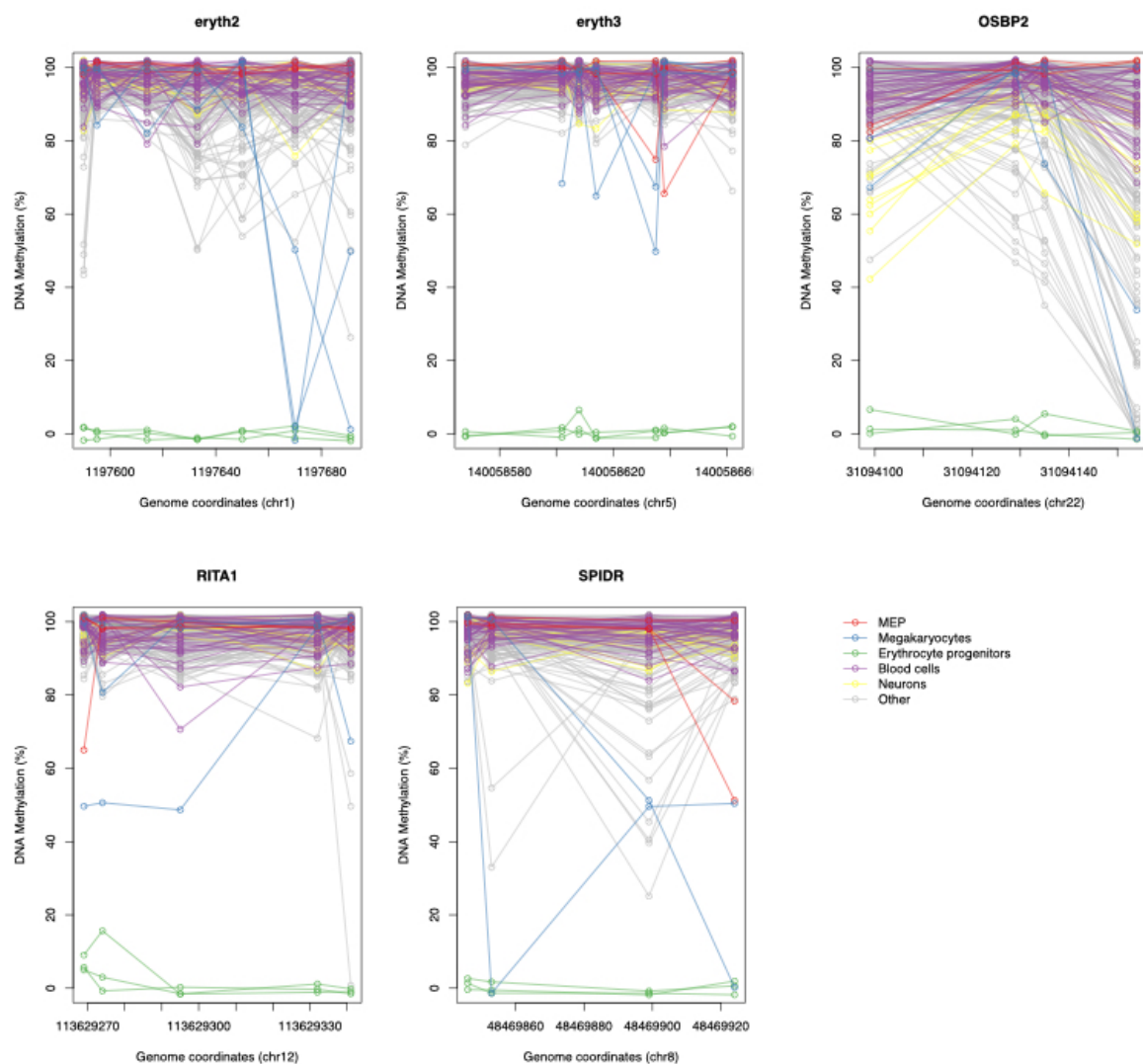


654
655 **Fig S2. Density plot of methylomes of hematopoietic lineage demonstrating global**
656 **demethylation in erythroblasts as compared to other cell types.**



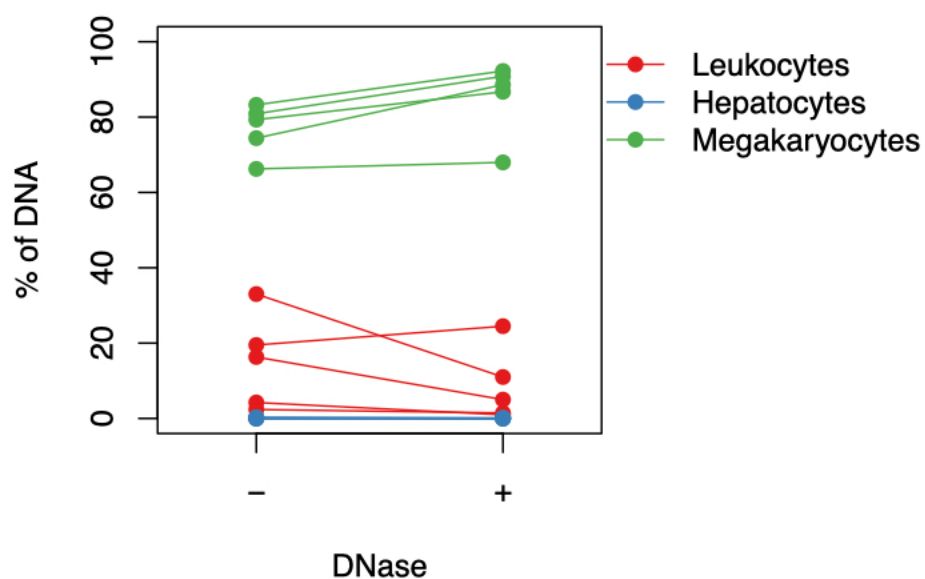
657
658
659
660
661

Fig S3. Megakaryocyte DNA methylation markers in megakaryocytes and other cell types.



662
663

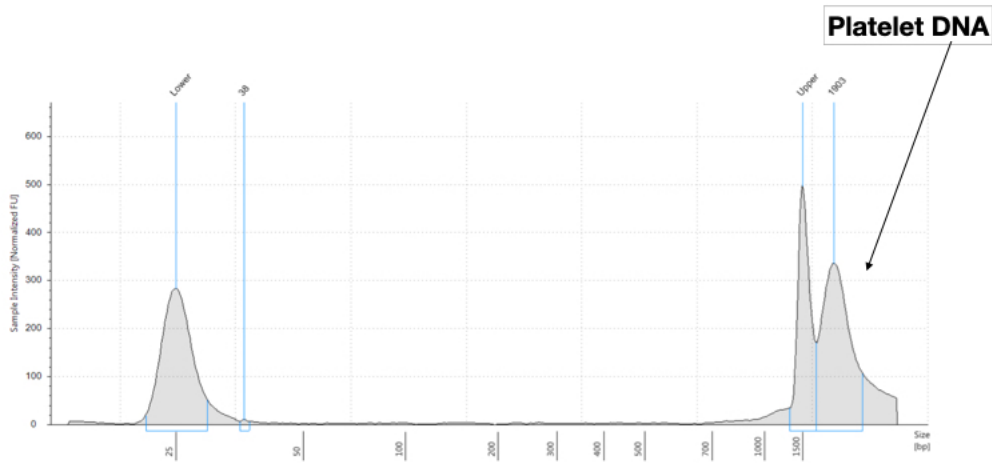
Fig S4. Erythroblast DNA methylation markers in megakaryocytes and other cell types.



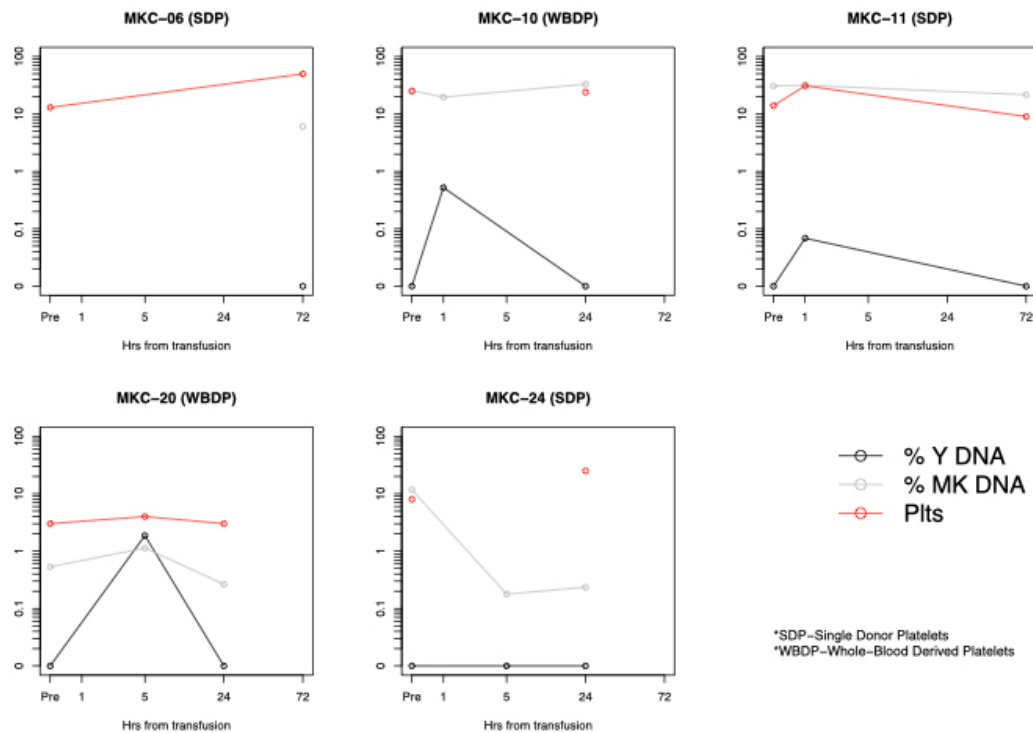
664
665

Fig S5. MK DNA in centrifuged platelets treated with DNase.

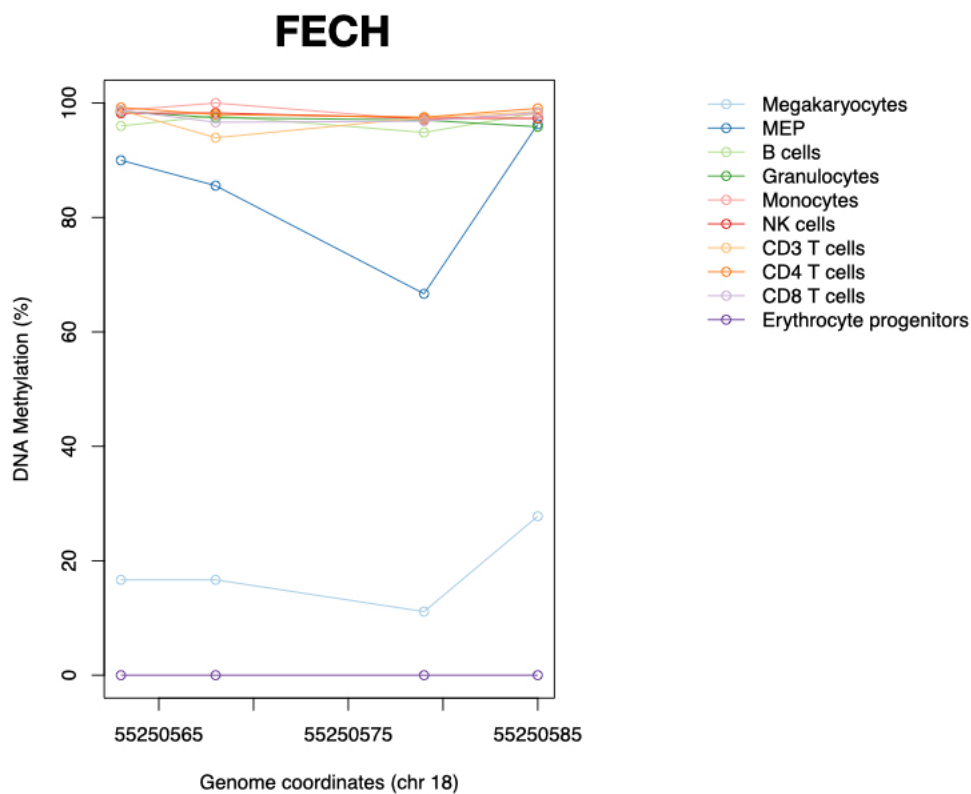
666 The percentage of MK DNA isolated from centrifuged platelets is significantly increased when
 667 treating with DNase, supporting the presence of MK DNA within platelets as opposed to
 668 leukocyte and liver DNA ($p < 0.05$).



669 **Fig S6. Platelet DNA is composed of high molecular weight DNA, as measured by Agilent**
 670 **High Sensitivity D1000 system.**
 671



672 **Fig S7. %Y chromosome DNA (SRY/b-Actin), platelet counts and MK DNA for females**
 673 **receiving male donor platelets.**
 674



675
676
677
678
679

Fig S8. A previously reported erythroid-specific unmethylated marker is unmethylated in both erythroblasts and megakaryocytes.